Ionization cross sections and probabilities for removal of $2s$ and $2p$ atomic electrons in the binary-encounter approximation

J. H. McGuire*† and K. Omidvar

Theoretical Studies Group, NASA-Goddard Space Flight Center, Greenbelt, Maryland 20771

(Received 7 December 1973; revised manuscript received 26 March 1974)

Calculations of ionization cross sections have been performed for removing electrons from $2s$ and $2p$ levels in hydrogenlike atoms by heavy-charged-particle impact using the binary-encounter approximation (BEA). The ratio of $\sigma_{L_{II}}/\sigma_{L_I}$ is predicted to peak when the projectile has a velocity equal to 0.3 times the velocity of the atomic electron. Experimental values of $\sigma_{L_{II}}/\sigma_{L_I}$, in agreement with Born predictions, peak at a velocity significantly lower than that predicted by BEA calculations. By transforming to coordinate space in an approximate way, predictions for the impact-parameter dependence are made. In the $2s$ case, the ionization probability has a pronounced local minimum for impact parameters near half the atomic radius, corresponding to a node in the $2s$ wave function. The ionization probabilities for arbitrary charged particles on arbitrary targets may be easily found by applying scaling laws to values tabulated over a wide range of projectile velocities.

I. INTRODUCTION

There are many ways to predict cross sections when a limited number of channels are open, and when the process may be considered as a two-body problem. Since neither of these criteria is easily met in the case of atomic ionization by heavy-charged-particle impact, it should not be surprising that few practical solutions exist, and that the existing solutions are rigorously valid only in certain regions, i.e., at high energies. Consequently, it is reasonable to develop and test models, particularly in regions where rigorous solutions do not exist, where data do exist, and where the model is relatively simple to use.

The binary-encounter approximation[1-3] (BEA), of course, is such a model, useful at low and intermediate projectile velocities where it is not clear that the Born[4,5] or Glauber[6] approximations rigorously apply. The cross sections obtained in the BEA model obey remarkably simple scaling laws suggesting that vacancy-production data for various projectiles and targets should have the same velocity dependence. Experimental data support this simple model to a remarkable degree, i.e., the data for ionization of inner-shell electrons by the impact of protons and α particles is usually within a factor of 2 of the BEA predictions (and Born predictions, as well) over a wide range of projectile velocities.

Recently, the BEA model has been extended[7,8] to predict the impact-parameter dependence of the ionization cross sections, i.e., to compute the probability of ionization as a function of the impact parameter of the projectile. In extending the model, at least two additional assumptions are introduced, namely, that (i) there exists an algebraic relationship between the velocity of the atomic electron and its distance from the nucleus; (ii) ionization occurs when the projectile and electron are separated by a distance small compared to the atomic radius. The predictions themselves are in good qualitative agreement with recent impact-parameter measurements for K-shell electrons. Furthermore, comparison with multiple K- and L-shell ionization[7,9] data supports predictions for the L shell near zero impact parameter.

While there has been considerable work done for filled atomic shells, little attention has been given to the subshell structure. Recently, Hansen[7] has computed cross sections for ionization in the $2s$ and $2p$ subshells. However, there has been no prediction of the impact-parameter dependence of the ionization probabilities for atomic subshells in either the BEA model nor any other model.

In Sec. II we formulate expressions for ionization cross sections and probabilities in the $2s$ and $2p$ subshells. In Sec. III, we compare our results to recent observations[10,11] of $\sigma_{L_{II}}/\sigma_{L_I}$ and $\sigma_{L_{III}}/\sigma_{L_{II}}$.

In Sec. IV, we present predictions for the ionization probability in the $2s$ and $2p$ subshells, each of which differs significantly from the prediction for filled shells. Applying the usual scaling laws for these probabilities to tabulated values, predictions for arbitrary targets and projectiles are easily found.

II. FORMULATION

In the BEA model, one approximates the ionization problem by considering a binary encounter

between a projectile and a free electron. The effective two body cross section, averaged over allowed energy transfers,[1,2] is then averaged over the density distribution for an atomic electron. The expression for the differential cross section, $d\sigma_{\rm eff}/d(\Delta E)dq$, has been derived by Bates and McDonough,[12] namely

$$\frac{d\sigma_{\rm eff}}{d(\Delta E)}\,dq=\frac{4\pi z^2Z^2e^4}{v_i^2\,q^4}\int\rho(v_2)v_2\,dv_2\,. \tag{1}$$

Here q is the momentum transfer, ΔE is the energy transferred to the target electron, z is the charge of the projectile, Z is the nuclear charge seen by the atomic electron, e is the charge of the electron, v_i is the projectile velocity, v_2 is the electron velocity, and $\rho(v_2)$ is the density distribution of the atomic electron. This expression is valid for arbitrary density distributions $\rho(v_2)$ in randomly oriented targets (e.g., no external electric or magnetic fields). The density distribution is normalized according to

$$\int_0^\infty\rho(v_2)v_2^2\,dv_2=1\,. \tag{2}$$

The total cross section may then be found by integrating Eq. (1) over allowed ranges[1,2] of energy and momentum transfers. It is important to note that the limits of integration depend on v_2.

For filled hydrogenic shells, the density distribution, corresponding to the square of the wave function in momentum[13] (or a microcononical statistical distribution of classical particles) is given by

$$\rho(v_2)=\frac{32}{\pi}\,\frac{v_0^5}{(v_2^2+v_0^2)^4}\,, \tag{3}$$

where the binding energy $-U=\frac{1}{2}mv_0^2$. In this case the total cross section for ionization is given by

$$\sigma(V)=\int_0^\infty\rho(v_2)v_2^2\,dv_2\int_U^{E_i}\frac{d\sigma_{\rm eff}}{d\Delta E}\,d(\Delta E)$$
$$=\frac{N_z^2\sigma_0}{U^2}\,G(V), \tag{4}$$

where N is the number of electrons in the filled shell, $V=v_i/v_0$ is the scaled velocity, $\sigma_0=6.56\times10^{-14}$ cm^{2}eV^2, and $G(V)$ is a tabulated[9] function of V. A closed form expression for $d\sigma_{\rm eff}/d(\Delta E)$ is given[3] by Garcia.

For the $2s$ subshell, the density distribution is given by

$$\rho_{2s}(v_2)=\frac{32}{\pi}\,\frac{v_0^5}{(v_2^2+v_0^2)^6}(v_2^2-v_0^2)^2\,. \tag{5}$$

Now the total cross section for removing electrons from the $2s$ level may be computed using Garcia's result[3] for $d\sigma_{\rm eff}/d(\Delta E)$, giving

TABLE I. $G(V)$ vs V for $2s$ and $2p$ electrons. The cross section for ionization is given by $\sigma(V)=Nz^2\sigma_0G(V)/U^2$. Here $N=2$ (or 6) for $2s$ (or $2p$), $\sigma_0=6.56\times10^{-14}$ cm^2 eV^2, U is the binding energy meV, and $V=(mE/MU)^{1/2}=v_i/v_0$ is the scaled velocity where the projectile energy $E=\frac{1}{2}mv_i^2$ and $|U|=\frac{1}{2}mv_0^2$. Hansen's tables (Ref. 7) of $U^2\sigma/N_z^2$ correspond to $\sigma_0G(V)\times10^{18}$. In our notation, $0.729(-4)=0.729\times10^{-4}$.

V	$G_{2s}(V)$	$G_{2p}(V)$
0.10	0.729(−4)	0.959(−5)
0.12	0.246(−3)	0.494(−4)
0.14	0.601(−3)	0.171(−3)
0.16	0.124(−2)	0.510(−3)
0.18	0.211(−2)	0.125(−2)
0.20	0.327(−2)	0.278(−2)
0.22	0.458(−2)	0.488(−2)
0.24	0.598(−2)	0.915(−2)
0.26	0.743(−2)	0.153(−1)
0.28	0.890(−2)	0.227(−1)
0.30	0.118(−1)	0.325(−1)
0.32	0.170(−1)	0.458(−1)
0.34	0.238(−1)	0.614(−1)
0.36	0.317(−1)	0.785(−1)
0.38	0.446(−1)	0.975(−1)
0.40	0.645(−1)	0.118
0.42	0.896(−1)	0.141
0.44	0.118	0.164
0.46	0.153	0.187
0.48	0.193	0.211
0.50	0.236	0.236
0.52	0.283	0.260
0.54	0.331	0.285
0.56	0.381	0.309
0.58	0.432	0.334
0.60	0.479	0.358
0.62	0.523	0.381
0.64	0.565	0.405
0.66	0.605	0.429
0.68	0.643	0.452
0.70	0.679	0.475
0.72	0.708	0.496
0.74	0.730	0.516
0.76	0.746	0.535
0.78	0.757	0.553
0.80	0.765	0.570
0.85	0.773	0.611
0.90	0.773	0.650
0.95	0.758	0.673
1.00	0.731	0.684
1.2	0.598	0.684
1.4	0.495	0.607
1.6	0.419	0.526
1.8	0.358	0.443
2.0	0.312	0.376
2.25	0.264	0.308
2.5	0.225	0.255
2.75	0.192	0.213
3.0	0.166	0.180

$$\sigma_{2s}(v) = \int_0^\infty \rho_{2s}(v_2) v_2^2 \, dv_2 \int_U^{E_i} \frac{d\sigma_{\text{eff}}}{d(\Delta E)} \, d(\Delta E)$$
$$= \frac{2z^2\sigma_0}{U^2} G_{2s}(v), \tag{6}$$

where $G_{2s}(v)$ is tabulated in Table I. Hansen's tables[7] of $U^2\sigma/Nz^2$ correspond to $\sigma_0 G(V)\times 10^{18}$.

Similarly, for $2p$ electrons where the density distribution is given by

$$\rho_{2p}(v_2) = \frac{32}{\pi} \frac{v_0^5}{(v_2^2+v_0^2)^6} \frac{4}{3} v_2^2 v_0^2, \tag{7}$$

the total cross section is given by

$$\sigma_{2p}(V) = \frac{6z^2\sigma_0 G_{2p}(V)}{U^2}, \tag{8}$$

where $G_{2p}(V)$ is also listed in Table I. We note that

$$2G_{2s}(V) + 6G_{2p}(V) = 8G(V), \tag{9}$$

corresponding[13] to $2\sigma_{2s} + 6\sigma_{2p} = 8\sigma_2$. These results may be easily used to compute total cross sections for ionization in the $2s$ and $2p$ levels.

In order to express the cross section in terms of the ionization probability, i.e.,

$$\sigma(V) = \int_0^\infty 2\pi b P(b, V) \, db, \tag{10}$$

we must transform to coordinate space. This may be done[7,8] by assuming that the electron velocity v_2 is a function of its distance from the nucleus, σ. This may be done classically, using conservation of energy, namely

$$\tfrac{1}{2} m v_2^2 - (Ze^2/r) = -\tfrac{1}{2} m v_0^2, \tag{11}$$

but this gives imaginary values of v_2 for $r > 2a = 2n/v_0$, where n is the principal quantum number. Instead we prefer Hansen's relation,[7]

$$\int_0^r \rho(r) r^2 \, dr + \int_0^{v_2} \rho(v_2) v_2^2 \, dv_2 = 1, \tag{12}$$

in accordance with the uncertainty principle. Here $\rho(r)$ is the coordinate space density distribution, and $\rho(v_2)$ is the velocity space distribution.

We may now express the cross section in the form of Eq. (8). Since $v_2 = v_2(r)$, we may write Eq. (4) as

$$\sigma(V) = \int_0^\infty \rho(r) r^2 \, dr \int \frac{d\sigma_{\text{eff}}(v_i, v_2(r))}{d(\Delta E)} \, d(\Delta E)$$
$$= (1/4\pi) \int_0^\infty \rho(r) \, d^3r \int \frac{d\sigma_{\text{eff}}}{d(\Delta E)} \, d(\Delta E)$$
$$= \int_0^\infty 2\pi b \, db \int_0^\infty \frac{\rho((b^2+z^2)^{1/2}) \, dz}{2\pi}$$
$$\times \int \frac{d\sigma_{\text{eff}}}{d(\Delta E)} \, d(\Delta E). \tag{13}$$

We now identify

$$P(b) = \int_0^\infty \frac{\rho((b^2+z^2)^{1/2}) \, dz}{2\pi} \int \frac{d\sigma_{\text{eff}}}{d(\Delta E)} \, d(\Delta E). \tag{14}$$

Here we have chosen $\rho(r)$ rather than $\rho(v_2(r))$ since using the former gives a correspondence[8] to the plane-wave Born approximation and better represents data for K-shell ionization. We have also assumed that b is the impact parameter of both the projectile and the atomic electron.

It has been previously pointed out[9] that, in the BEA model, the ionization probability satisfies remarkably simple scaling properties, namely that

$$P(b, V) = (z/Z)^2 P(b/a, V), \tag{15}$$

where $P(b/a, V)$ has been tabulated[8] for ionization in the K shell. Here a is the radius of the atomic electron. In Sec. IV we tabulate $P_{2s}(b/a)$ and $P_{2s}(b/a, V)$.

III. CROSS-SECTION RATIOS

In order to compare the results of Sec. II to experimental x-ray measurements, it is necessary to transform from $2s, 2p$ notation to L_{I}, L_{II}, L_{III} notation. The (n, l, n_l, s, m_s) wave functions may be related to the (n, j, m_j, s, m_s) wave functions using Clebsch-Gordan coefficients. Since the density distributions are just the square of the wave functions, it is straightforward to derive the obvious relations,

$$\rho_{L_{\text{I}}} = \rho_{2s}, \quad \rho_{L_{\text{II}}} = \rho_{L_{\text{III}}} = \rho_{2p}. \tag{16}$$

The binding energies for L_{I}, L_{II}, and L_{III} differ from one another. Consequently, at a fixed pro-

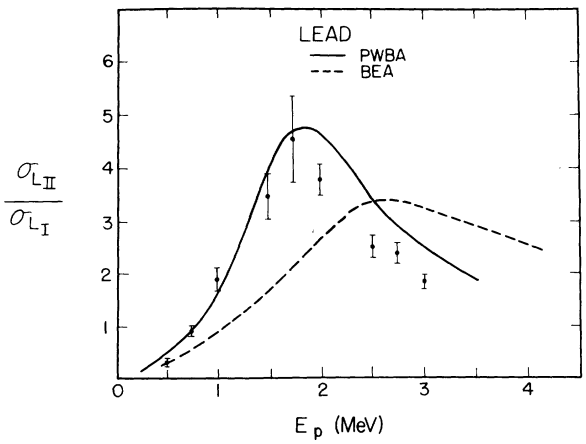

FIG. 1. Ratio of $\sigma_{L_{\text{II}}}/\sigma_{L_{\text{I}}}$ vs projectile energy for p+Pb. The plane-wave Born-approximation (PWBA) calculation is from Merzbacher *et al.* (Ref. 4). The data were taken by Shafroth *et al.*

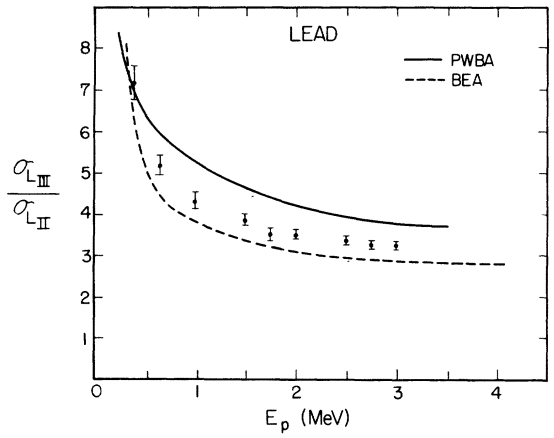

FIG. 2. Ratio of $\sigma_{L_{III}}/\sigma_{L_{II}}$ vs projectile energy for p+Pb. At the same scaled velocity, the BEA model predicts that the ratio is 2. At a fixed projectile energy, deviations from two are due to differences in the binding energies for L_{II} and L_{III} electrons.

jectile velocity, the scaled velocities are different for each subshell. Therefore, $\sigma_{L_{II}}$ and $\sigma_{L_{III}}$ are not identical at fixed projectile velocity. Furthermore, the subshell sum ruled defined by Eq. (9) is broken. In most instances, the subshell binding energies are similar, and the differences which we have just discussed are small.

Recently there have been observations of the ratio of $\sigma_{L_{II}}/\sigma_{L_I}$ in atoms near[10] $Z=80$ and near[11] $Z=60$ over a range of projectile energies. In Fig. 1 we compare the BEA results to the observations of the group[10] in North Carolina, and to predictions by Merzbacher.[4] Our BEA results (shown) differ by 20% or so from those quoted by Madison *et al.* (not shown). In any case, the Born results tend to predict the position of the peak more accurately than do the BEA results. In our calculations we find that the position and magnitude of the peak is a sensitive function of the scaled velocity, so that these measurements tend to emphasize delicate features of the total cross sections.

In Fig. 2 we compare the BEA prediction for $\sigma_{L_{III}}/\sigma_{L_{II}}$ to experiment and to the Born calculation. In the BEA prediction, the increase in $\sigma_{L_{III}}/\sigma_{L_{II}}$ at low energies reflects the sensitivity of $G_{2p}(V)$ to small changes in V due to differences in the subshell binding energies $U_{L_{II}}$ and $U_{L_{III}}$. In this case the BEA predictions seem closer to experiment than the Born predictions.

In Fig. 3 we predict a universal curve for $\sigma_{L_I}/\sigma_{L_I}$ for fixed scaled velocity. Here, one must vary the projectile velocity, so that the scaled velocity, $V=(Em/UM)^{1/2}$ remains the same. This curve has a sharp local maximum at $V=0.30$ and a broad local minimum at $V=0.70$. According to our BEA predictions, the ratio $\sigma_{L_{III}}/\sigma_{L_{II}}=2$ at fixed scaled velocity.

IV. IONIZATION PROBABILITIES

Previous BEA calculations[7-9] of the ionization probability indicate that the probability is essentially a monotonically decreasing function of impact parameter for filled shells. Born calculations and observations for ionization in the K shell agree with the BEA predictions and with each other within ~50%.

In Fig. 4 we present the ionization probability for $2s$ and $2p$ electrons at $V=1$. The dominant feature in both cases is that the impact parameter dependence is markedly different from the monotonic dependence for filled shells. In the $2s$ cal-

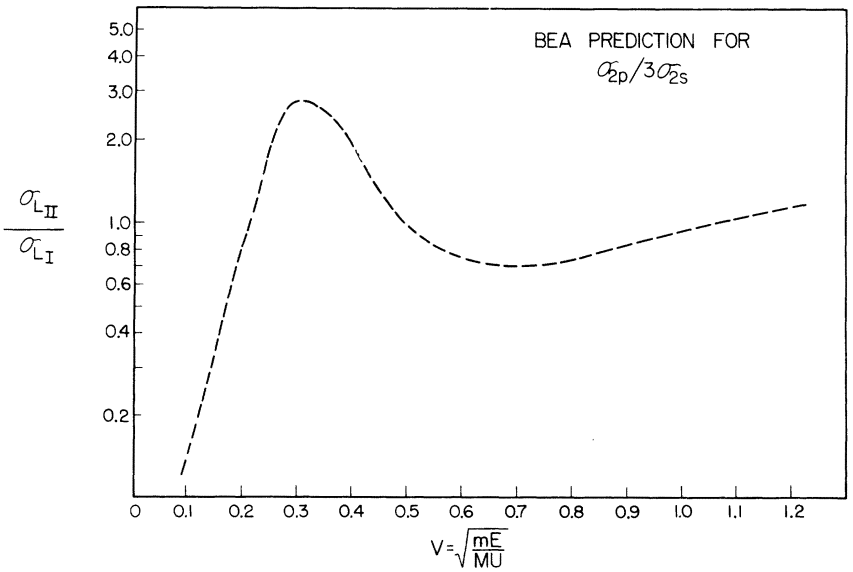

FIG. 3. Ratio of $\sigma_{L_{II}}/\sigma_{L_I}$ vs projectile energy at fixed scaled velocity. According to the BEA model, cross-section ratios for all targets and projectiles taken at the same scaled velocity should lie on this curve. The maximum occurs at $V=0.30$ and the minimum at $V=0.70$.

culations there is a local minimum near $b = \frac{1}{2}a$, corresponding to a node in the $2s$ radial wave function at $b = \frac{1}{2}a$. In the $2p$ case, there is a maximum near $b = a$, again due to a maximum in the $2p$ density distribution. The sum of twice the $2s$ probability plus six times the $2p$ probability gives an impact parameter dependence which monotonically decreases. However, in coordinate space the density distributions do not satisfy the sum rule [Eq. (9)] for filled shells satisfied by velocity space density distributions.

Comparing Fig. 4 and Fig. 5 we see that the minor variations in the $2s$ values of $P(b)$ correspond to variations in the kinematics near $b = \frac{1}{2}a$. Since such variations are not present for the $2p$ shell in either $P(b)$ or the kinematics, we attribute these $2s$ minor variations to kinematics. Since these fluctuations appear to be due to Hansen's kinematics, and since we have no correct kinematics in our classical approach, we find it difficult to state definitively whether or not the minor fluctuations are correct. In our opinion they are probably spurious. However, especially since a quantum mechanical calculation[13] is feasible, we see little point in stating a definitive conclusion in this matter. Furthermore, these minor fluctuations seem to be comparable to experimental error with existing experimental technique. Consequently, we leave the question somewhat open.

In Tables II and III we present tabulated values of $P(b, V)$ for the $2s$ and $2p$ subshells. The ionization probability for projectiles of charge z incident on an atomic electron bound by a nuclear charge $Z = n(U/13.6)^{1/2}$, is given by $(z/Z)^2 P(V, b)$.

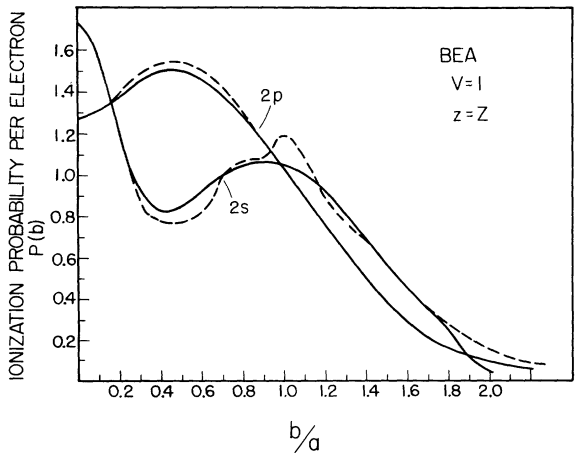

FIG. 4. Probability for ionization in the $2s$ and $2p$ subshells as a function of impact parameter at $V = 1$. The minimum in the $2s$ curve occurs at $b = \frac{1}{2}a$, corresponding to the node in the radial wave function for $2s$ electrons. The solid curves employ Eq. (11) while the dashed curves use Eq. (12) due to Hansen. The two approximations give similar results except at large impact parameters.

V. DISCUSSION

In the BEA model, cross sections are computed using a single parameter, namely the binding energy U which may be determined experimentally in most cases. In the Born approximation, two parameters are adjusted to correspond to experimental values, namely the binding energy U and the effective nuclear charge Z. Furthermore, the less rigorous BEA model corresponds to the Born approximation in the limit of high velocities of the ejected electron. Consequently, it should come as no surprise that the Born approximation gives somewhat better agreement with the $\sigma_{L_{II}}/\sigma_{L_I}$ experimental data than does the BEA model. If there is any surprise, it is that these approximations work at all in this low energy region. In the same vein, one should view with caution predictions of universal curves such as Fig. 3, since many simplifying assumptions have been made in order to produce such a curve. At best such results can be expected to reflect a general trend to be looked for in experimental data.

In Sec. II we pointed out that to compute total cross sections in coordinate space required more assumptions than are required in velocity space. In our calculations we have chosen the density distribution equal to the square of the wave function, i.e.,

$$\rho_{ni}(\vec{r}) = |\Psi_{ni}(\vec{r})|^2 = \left| \int d\vec{p}\, e^{i\vec{p}\cdot\vec{r}} \Psi_{ni}(\vec{p}) \right|^2 .$$

Such a choice preserves the correspondence[8] to

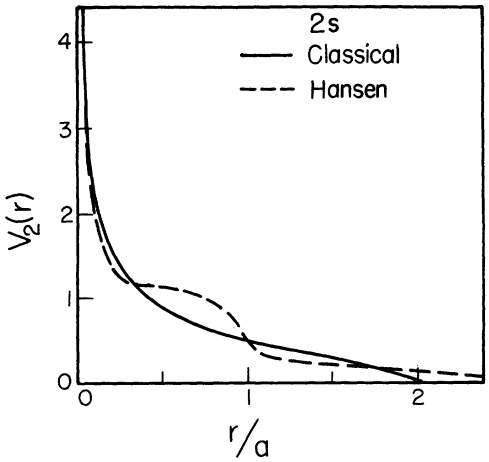

FIG. 5. Velocity-distance diagram for the $2s$ subshell; the solid curve is classical [Eq. (11)] and the broken curve is due to Hansen [Eq. (12)]. For the $2p$ subshell, Hansen's result is very close to the classical result.

TABLE II. Ionization probabilities per electron for $2s$ subshells as a function of impact parameter b and scaled velocity V, for $z=Z$. The impact parameter b is given in units of the electron radius, $a=4a_0/Z$. Z is the effective target charge, equal to $4|U_L|/13.6$, where U_L is the L shell binding energy in eV. The coordinate-space hydrogenic L-shell electron density distribution is used, along with Hansen's transformation given by Eq. (12). To use the table, compute $V=(mE_i/MU)^{1/2}$, find $P(b)$ from the table and multiply by $(z/Z)^2$, where z is the charge of the projectile. In our notation, $0.323(-1)=0.323\times10^{-1}$.

V \ b	0.05	0.1	0.2	0.3	0.4	0.5	0.6	0.7	0.8	0.9	1.0	1.1	1.2	1.3	1.4	1.6	1.8	2.0	2.5
0.10	0.323(−1)	0.162(−1)	0.863(−3)																
0.12	0.525(−1)	0.328(−1)	0.704(−2)	0.914(−3)	0.716(−4)	0.571(−4)	0.122(−3)	0.224(−4)											
0.14	0.757(−1)	0.540(−1)	0.178(−1)	0.432(−2)	0.764(−3)	0.333(−3)	0.994(−3)	0.102(−2)	0.173(−3)										
0.16	0.102(0)	0.771(−1)	0.310(−1)	0.998(−2)	0.352(−2)	0.204(−2)	0.235(−2)	0.329(−2)	0.217(−2)	0.154(−3)									
0.18	0 127(0)	0.101(0)	0.453(−1)	0.167(−1)	0.746(−2)	0.586(−2)	0.559(−2)	0.613(−2)	0.571(−2)	0.151(−2)								2S	
0.20	0.153(0)	0.125(0)	0.598(−1)	0.239(−1)	0.120(−1)	0.108(−1)	0.113(−1)	0.925(−2)	0.100(−1)	0.532(−2)									
0.22	0.179(0)	0.149(0)	0.744(−1)	0.312(−1)	0.168(−1)	0.162(−1)	0.183(−1)	0.125(−1)	0.147(−1)	0.107(−1)									
0.24	0.205(0)	0.172(0)	0.888(−1)	0.385(−1)	0.217(−1)	0.219(−1)	0.260(−1)	0.157(−1)	0.196(−1)	0.169(−1)									
0.26	0.230(0)	0.195(0)	0.103(0)	0.458(−1)	0.266(−1)	0.277(−1)	0.341(−1)	0.205(−1)	0.246(−1)	0.236(−1)	0.489(−3)								
0.28	0.255(0)	0.218(0)	0.117(0)	0.530(−1)	0.315(−1)	0.335(−1)	0.424(−1)	0.292(−1)	0.306(−1)	0.305(−1)	0.402(−2)	0.821(−4)							
0.30	0.279(0)	0.240(0)	0.131(0)	0.602(−1)	0.364(−1)	0.393(−1)	0.507(−1)	0.407(−1)	0.411(−1)	0.395(−1)	0.115(−1)	0.321(−2)	0.197(−3)						
0.32	0.308(0)	0.267(0)	0.148(0)	0.700(−1)	0.432(−1)	0.460(−1)	0.592(−1)	0.539(−1)	0.549(−1)	0.532(−1)	0.252(−1)	0.115(−1)	0.399(−2)	0.684(−3)					
0.34	0.341(0)	0.298(0)	0.170(0)	0.848(−1)	0.550(−1)	0.574(−1)	0.717(−1)	0.709(−1)	0.720(−1)	0.701(−1)	0.447(−1)	0.271(−1)	0.143(−1)	0.623(−2)	0.187(−2)				
0.36	0.378(0)	0.332(0)	0.196(0)	0.103(0)	0.705(−1)	0.728(−1)	0.884(−1)	0.931(−1)	0.950(−1)	0.926(−1)	0.699(−1)	0.490(−1)	0.316(−1)	0.190(−1)	0.945(−2)	0.833(−3)			
0.38	0.417(0)	0.369(0)	0.224(0)	0.125(0)	0.893(−1)	0.914(−1)	0.108(0)	0.119(0)	0.122(0)	0.120(0)	0.102(0)	0.781(−1)	0.565(−1)	0.388(−1)	0.238(−1)	0.482(−2)	0.829(−3)		
0.40	0.461(0)	0.411(0)	0.258(0)	0.151(0)	0.113(0)	0.114(0)	0.132(0)	0.149(0)	0.154(0)	0.153(0)	0.139(0)	0.113(0)	0.876(−1)	0.652(−1)	0.451(−1)	0.182(−1)	0.554(−2)	0.772(−3)	
0.44	0.559(0)	0.504(0)	0.334(0)	0.213(0)	0.169(0)	0.171(0)	0.191(0)	0.221(0)	0.175(0)	0.230(0)	0.226(0)	0.198(0)	0.166(0)	0.134(0)	0.104(0)	0.573(−1)	0.281(−1)	0.118(−1)	0.480(−3)
0.50	0.723(0)	0.660(0)	0.465(0)	0.324(0)	0.271(0)	0.144(0)	0.297(0)	0.347(0)	0.361(0)	0.366(0)	0.380(0)	0.235(0)	0.308(0)	0.264(0)	0.220(0)	0.143(0)	0.872(−1)	0.500(−1)	0.104(−1)
0.60	0.101(1)	0.934(0)	0.697(0)	0.525(0)	0.457(0)	0.460(0)	0.490(0)	0.573(0)	0.597(0)	0.394(0)	0.653(0)	0.621(0)	0.568(0)	0.504(0)	0.439(0)	0.314(0)	0.213(0)	0.138(0)	0.410(−1)
0.70	0.128(1)	0.119(1)	0.915(0)	0.711(0)	0.628(0)	0.632(0)	0.688(0)	0.781(0)	0.814(0)	0.835(0)	0.707(0)	0.871(0)	0.808(0)	0.726(0)	0.640(0)	0.468(0)	0.318(0)	0.202(0)	0.533(−1)
0.80	0.149(1)	0.139(1)	0.108(1)	0.840(0)	0.745(0)	0.749(0)	0.792(0)	0.934(0)	0.975(0)	0.998(0)	0.109(1)	0.105(1)	0.977(0)	0.873(0)	0.757(0)	0.522(0)	0.335(0)	0.205(0)	0.520(−1)
0.90	0.165(1)	0.154(1)	0.118(1)	0.905(0)	0.795(0)	0.791(0)	0.831(0)	0.999(0)	0.105(1)	0.108(1)	0.119(1)	0.113(1)	0.102(1)	0.881(0)	0.740(0)	0.493(0)	0.310(0)	0.187(0)	0.470(−1)
1.00	0.172(1)	0.160(1)	0.120(1)	0.892(0)	0.771(0)	0.770(0)	0.821(0)	0.102(1)	0.107(1)	0.107(1)	0.119(1)	0.109(1)	0.952(0)	0.809(0)	0.672(0)	0.442(0)	0.276(0)	0.166(0)	0.415(−1)
1.20	0.181(1)	0.167(1)	0.118(1)	0.825(0)	0.689(0)	0.700(0)	0.779(0)	0.942(0)	0.950(0)	0.966(0)	0.100(1)	0.880(0)	0.756(0)	0.637(0)	0.526(0)	0.343(0)	0.214(0)	0.128(0)	0.318(−1)
1.40	0.192(1)	0.175(1)	0.119(1)	0.778(0)	0.627(0)	0.651(0)	0.757(0)	0.807(0)	0.836(0)	0.882(0)	0.792(0)	0.691(0)	0.592(0)	0.498(0)	0.411(0)	0.267(0)	0.166(0)	0.995(−1)	0.247(−1)
1.60	0.206(1)	0.187(1)	0.123(1)	0.758(0)	0.591(0)	0.626(0)	0.753(0)	0.704(0)	0.757(0)	0.805(0)	0.631(0)	0.549(0)	0.470(0)	0.395(0)	0.326(0)	0.212(0)	0.132(0)	0.789(−1)	0.196(−1)
1.80	0.222(1)	0.200(1)	0.128(1)	0.758(0)	0.574(0)	0.618(0)	0.674(0)	0.634(0)	0.709(0)	0.688(0)	0.510(0)	0.444(0)	0.380(0)	0.319(0)	0.263(0)	0.171(0)	0.106(0)	0.637(−1)	0.158(−1)
2.00	0.239(1)	0.215(1)	0.207(1)	0.773(0)	0.561(0)	0.547(0)	0.594(0)	0.587(0)	0.642(0)	0.572(0)	0.420(0)	0.366(0)	0.313(0)	0.263(0)	0.217(0)	0.141(0)	0.876(−1)	0.524(−1)	0.130(−1)
2.50	0.279(1)	0.247(1)	0.146(1)	0.703(0)	0.401(0)	0.379(0)	0.437(0)	0.431(0)	0.432(0)	0.376(0)	0.275(0)	0.239(0)	0.205(0)	0.172(0)	0.142(0)	0.922(−1)	0.574(−1)	0.344(−1)	0.852(−2)
3.00	0.289(1)	0.256(1)	0.134(1)	0.507(0)	0.283(0)	0.267(0)	0.308(0)	0.304(0)	0.303(0)	0.264(0)	0.193(0)	0.168(0)	0.144(0)	0.121(0)	0.996(−1)	0.648(−1)	0.403(−1)	0.241(−1)	0.599(−2)
3.50	0.308(1)	0.273(1)	0.999(0)	0.375(0)	0.209(0)	0.197(0)	0.227(0)	0.224(0)	0.224(0)	0.195(0)	0.143(0)	0.124(0)	0.106(0)	0.894(−1)	0.737(−1)	0.480(−1)	0.298(−1)	0.179(−1)	0.444(−2)
4.00	0.332(1)	0.259(1)	0.768(0)	0.288(0)	0.160(0)	0.151(0)	0.175(0)	0.172(0)	0.172(0)	0.150(0)	0.110(0)	0.956(−1)	0.818(−1)	0.688(−1)	0.567(−1)	0.369(−1)	0.230(−1)	0.138(−1)	0.341(−2)
5.00	0.333(1)	0.167(1)	0.493(0)	0.185(0)	0.103(0)	0.971(−1)	0.112(0)	0.111(0)	0.111(0)	0.962(−1)	0.706(−1)	0.615(−1)	0.526(−1)	0.443(−1)	0.365(−1)	0.237(−1)	0.148(−1)	0.885(−2)	0.220(−2)

TABLE III. Ionization probabilities per electron for $2p$ subshells. To use the table, compute $V=(mE_i/MU)^{1/2}$, find $P(b)$ from the table, and multiply by $(z/Z)^2$. In our notation, $0.302(-3)=0.302\times10^{-3}$.

V \ b	0.05	0.1	0.2	0.3	0.4	0.5	0.6	0.7	0.8	0.9	1.0	1.1	1.2	1.3	1.4	1.6	1.8	2.0	2.5
0.10	0.302(−3)	0.545(−3)	0.644(−3)																
0.12	0.199(−2)	0.207(−2)	0.197(−2)	0.766(−3)															
0.14	0.624(−2)	0.625(−2)	0.665(−2)	0.394(−2)	0.949(−3)														
0.16	0.114(−1)	0.117(−1)	0.136(−1)	0.114(−1)	0.630(−2)	0.154(−2)	0.751(−4)												
0.18	0.174(−1)	0.179(−1)	0.216(−1)	0.210(−1)	0.161(−1)	0.894(−2)	0.294(−2)	0.219(−3)											
0.20	0.291(−1)	0.297(−1)	0.347(−1)	0.344(−1)	0.292(−1)	0.205(−1)	0.118(−1)	0.463(−2)	0.805(−3)									$2P$	
0.22	0.455(−1)	0.462(−1)	0.530(−1)	0.540(−1)	0.491(−1)	0.386(−1)	0.262(−1)	0.148(−1)	0.696(−2)	0.190(−2)	0.942(−4)								
0.24	0.645(−1)	0.655(−1)	0.743(−1)	0.771(−1)	0.733(−1)	0.624(−1)	0.477(−1)	0.322(−1)	0.192(−1)	0.923(−2)	0.344(−2)	0.663(−3)							
0.26	0.870(−1)	0.881(−1)	0.988(−1)	0.103(0)	0.101(0)	0.898(−1)	0.736(−1)	0.552(−1)	0.381(−1)	0.234(−1)	0.124(−1)	0.552(−2)	0.178(−2)	0.226(−3)					
0.28	0.114(0)	0.115(0)	0.128(0)	0.134(0)	0.133(0)	0.122(0)	0.104(0)	0.828(−1)	0.618(−1)	0.427(−1)	0.270(−1)	0.160(−1)	0.808(−2)	0.328(−2)	0.964(−3)				
0.30	0.144(0)	0.145(0)	0.159(0)	0.168(0)	0.168(0)	0.158(0)	0.139(0)	0.115(0)	0.904(−1)	0.669(−1)	0.463(−1)	0.309(−1)	0.188(−1)	0.105(−1)	0.528(−2)	0.607(−3)			
0.32	0.176(0)	0.177(0)	0.193(0)	0.204(0)	0.206(0)	0.196(0)	0.176(0)	0.150(0)	0.122(0)	0.949(−1)	0.699(−1)	0.501(−1)	0.337(−1)	0.214(−1)	0.129(−1)	0.357(−2)	0.454(−3)		
0.34	0.210(0)	0.212(0)	0.230(0)	0.242(0)	0.246(0)	0.237(0)	0.216(0)	0.188(0)	0.157(0)	0.126(0)	0.964(−1)	0.723(−1)	0.516(−1)	0.355(−1)	0.237(−1)	0.896(−2)	0.249(−2)	0.411(−3)	
0.36	0.245(0)	0.248(0)	0.267(0)	0.282(0)	0.287(0)	0.279(0)	0.258(0)	0.228(0)	0.194(0)	0.159(0)	0.125(0)	0.970(−1)	0.721(−1)	0.521(−1)	0.367(−1)	0.164(−1)	0.625(−2)	0.190(−2)	
0.38	0.282(0)	0.285(0)	0.306(0)	0.323(0)	0.340(0)	0.322(0)	0.301(0)	0.269(0)	0.232(0)	0.194(0)	0.156(0)	0.123(0)	0.944(−1)	0.705(−1)	0.516(−1)	0.256(−1)	0.114(−1)	0.448(−2)	0.161(−3)
0.40	0.319(0)	0.323(0)	0.345(0)	0.365(0)	0.373(0)	0.366(0)	0.344(0)	0.311(0)	0.271(0)	0.229(0)	0.188(0)	0.151(0)	0.118(0)	0.903(−1)	0.679(−1)	0.360(−1)	0.177(−1)	0.798(−2)	0.687(−3)
0.44	0.395(0)	0.399(0)	0.425(0)	0.449(0)	0.460(0)	0.455(0)	0.432(0)	0.396(0)	0.351(0)	0.302(0)	0.254(0)	0.202(0)	0.168(0)	0.132(0)	0.103(0)	0.594(−1)	0.324(−1)	0.169(−1)	0.269(−2)
0.50	0.508(0)	0.514(0)	0.544(0)	0.575(0)	0.591(0)	0.588(0)	0.539(0)	0.523(0)	0.470(0)	0.412(0)	0.354(0)	0.296(0)	0.244(0)	0.198(0)	0.158(0)	0.975(−1)	0.576(−1)	0.328(−1)	0.710(−2)
0.60	0.692(0)	0.700(0)	0.738(0)	0.779(0)	0.802(0)	0.803(0)	0.777(0)	0.730(0)	0.664(0)	0.592(0)	0.517(0)	0.440(0)	0.370(0)	0.307(0)	0.251(0)	0.162(0)	0.101(0)	0.612(−1)	0.158(−1)
0.70	0.869(0)	0.879(0)	0.925(0)	0.976(0)	0.101(1)	0.101(1)	0.981(0)	0.928(0)	0.850(0)	0.763(0)	0.672(0)	0.577(0)	0.340(0)	0.411(0)	0.291(0)	0.224(0)	0.143(0)	0.887(−1)	0.240(−1)
0.80	0.744(0)	0.105(1)	0.110(1)	0.116(1)	0.120(1)	0.121(1)	0.118(1)	0.112(1)	0.103(1)	0.925(0)	0.818(0)	0.705(0)	0.602(0)	0.507(0)	0.420(0)	0.279(0)	0.179(0)	0.109(0)	0.261(−1)
0.90	0.119(1)	0.121(1)	0.126(1)	0.134(1)	0.138(1)	0.139(1)	0.135(1)	0.128(1)	0.803(0)	0.107(1)	0.948(0)	0.818(0)	0.697(0)	0.584(0)	0.483(0)	0.314(0)	0.189(0)	0.108(0)	0.244(−1)
1.00	0.132(1)	0.134(1)	0.141(1)	0.149(1)	0.154(1)	0.155(1)	0.151(1)	0.143(1)	0.132(1)	0.829(0)	0.105(1)	0.900(0)	0.760(0)	0.628(0)	0.503(0)	0.304(0)	0.176(0)	0.991(−1)	0.218(−1)
1.20	0.148(1)	0.150(1)	0.158(1)	0.167(1)	0.174(1)	0.175(1)	0.171(1)	0.112(1)	0.147(1)	0.130(1)	0.110(1)	0.891(0)	0.705(0)	0.549(0)	0.424(0)	0.247(0)	0.140(0)	0.778(−1)	0.169(−1)
1.40	0.156(1)	0.158(1)	0.168(1)	0.179(1)	0.185(1)	0.183(1)	0.175(1)	0.162(1)	0.141(1)	0.115(1)	0.921(0)	0.728(0)	0.567(0)	0.438(0)	0.336(0)	0.194(0)	0.110(0)	0.608(−1)	0.132(−1)
1.60	0.152(1)	0.153(1)	0.163(1)	0.172(1)	0.178(1)	0.178(1)	0.167(1)	0.142(1)	0.117(1)	0.938(0)	0.742(0)	0.584(0)	0.453(0)	0.349(0)	0.268(0)	0.154(0)	0.869(−1)	0.482(−1)	0.104(−1)
1.80	0.137(1)	0.138(1)	0.151(1)	0.162(1)	0.172(1)	0.164(1)	0.142(1)	0.117(1)	0.955(0)	0.763(0)	0.603(0)	0.473(0)	0.367(0)	0.283(0)	0.217(0)	0.125(0)	0.703(−1)	0.390(−1)	0.842(−2)
2.00	0.125(1)	0.127(1)	0.142(1)	0.156(1)	0.156(1)	0.139(1)	0.118(1)	0.969(0)	0.788(0)	0.629(0)	0.497(0)	0.390(0)	0.302(0)	0.233(0)	0.178(0)	0.103(0)	0.578(−1)	0.321(−1)	0.693(−2)
2.50	0.108(1)	0.109(1)	0.116(1)	0.119(1)	0.107(1)	0.921(0)	0.773(0)	0.635(0)	0.516(0)	0.412(0)	0.325(0)	0.255(0)	0.198(0)	0.152(0)	0.117(0)	0.671(−1)	0.379(−1)	0.210(−1)	0.454(−2)
3.00	0.788(0)	0.788(0)	0.884(0)	0.852(0)	0.754(0)	0.647(0)	0.542(0)	0.446(0)	0.362(0)	0.289(0)	0.228(0)	0.179(0)	0.139(0)	0.107(0)	0.819(−1)	0.472(−1)	0.266(−1)	0.148(−1)	0.319(−2)
3.50	0.587(0)	0.592(0)	0.685(0)	0.630(0)	0.557(0)	0.477(0)	0.401(0)	0.329(0)	0.267(0)	0.213(0)	0.169(0)	0.132(0)	0.103(0)	0.791(−1)	0.606(−1)	0.349(−1)	0.197(−1)	0.109(−1)	0.236(−2)
4.00	0.456(0)	0.465(0)	0.527(0)	0.484(0)	0.428(0)	0.367(0)	0.308(0)	0.253(0)	0.205(0)	0.164(0)	0.130(0)	0.102(0)	0.789(−1)	0.608(−1)	0.466(−1)	0.268(−1)	0.151(−1)	0.840(−2)	0.182(−2)
5.00	0.302(0)	0.316(0)	0.338(0)	0.311(0)	0.274(0)	0.235(0)	0.198(0)	0.162(0)	0.132(0)	0.105(0)	0.832(−1)	0.654(−1)	0.507(−1)	0.391(−1)	0.299(−1)	0.173(−1)	0.973(−2)	0.540(−2)	0.117(−2)

the Born approximation. Hansen, on the other hand, chooses[7] a different density distribution corresponding to

$$\rho_{nl}(\vec{r}) = \int d\vec{p}\, e^{i\vec{p}\cdot\vec{r}} |\Psi_{nl}(\vec{p})|^2 .$$

In this way Hansen preserves Fock's[14] sum rule, namely that $\sum_l \rho_{nl}$ is independent of n, which our choice fails to satisfy. However, Hansen's choice leads to wave functions in coordinate space which are not hydrogenic. Fortunately the differences in the ionization probabilities and cross sections are usually small compared to the over-all accuracy of the BEA model itself. Unless one is searching for a fine detail, or is at low velocities, it makes little difference which method is used. Except when one is forced to work in coordinate space (e.g., computation of ionization probabilities), it is preferable to work in velocity space (e.g., total cross sections) where these ambiguities do not arise.

Since we have seen that the local minimum in $P(b)$ for $2s$ electrons corresponds to a node in the radial wave function, it seems reasonable to expect that the BEA model will predict $n-l-1$ local minima in general corresponding to the $n-l-1$ nodes in $\Psi_{nl}(r)$ for higher shells.

Finally, we should like to point out that there exist no data on the impact parameter dependence of L-subshell ionization cross sections. Nor have there been calculations done in the Born approximation, although appropriate expressions[13] exist. Such measurements and calculations will provide a further test of the atomic ionization cross sections.

ACKNOWLEDGMENTS

We wish to thank S. M. Shafroth, T. Gray, and C. L. Cocke for several useful communications. One of the authors (J.H.M.) wishes to thank the members of the Theoretical Studies Branch at Goddard Space Flight Center for their hospitality.

---

*Permanent address: Department of Physics, Kansas State University, Manhattan, Kansas 66506.
†NASA/ASEE Summer Fellow.

[1]L. Vriens, *Case Studies in Atomic Physics I*, edited by E. W. McDaniel and M. R. C. McDowell (North-Holland, Amsterdam, 1970), Chap. 6.
[2]E. Gerjuoy, Phys. Rev. 148, 54 (1966).
[3]J. D. Garcia, Phys. Rev. A 1, 280 (1970); J. D. Garcia, Phys. Rev. A 4, 955 (1971); J. D. Garcia, E. Gerjuoy, and J. Welker, Phys. Rev. 165, 66 (1968).
[4]E. Merzbacher, *Proceedings of the International Conference on Inner Shell Ionization Phenomena, Atlanta, Georgia, 1973*, edited by R. W. Fink *et al.* (U.S. AEC, Oak Ridge, Tenn., 1973); G. S. Kendelwal, B. H. Choi, and E. Merzbacher, At. Data 1, 103 (1969); E. Merzbacher and W. H. Lewis, *Handbuch der Physik* (Springer, Berlin, 1958), Vol. 34, p. 166.
[5]K. Omidvar, Phys. Rev. 140, A26 (1965); K. Omidvar, H. L. Kyle, and E. C. Sullivan, Phys. Rev. A 5, 1175 (1972).
[6]J. H. McGuire, M. B. Hidalgo, G. D. Doolen and J. Nuttall, Phys. Rev. A 7, 973 (1973).
[7]J. S. Hansen, Phys. Rev. A 8, 822 (1973).
[8]J. H. McGuire, Phys. Rev. A 9, 286 (1974).
[9]J. H. McGuire and P. Richard, Phys. Rev. A 8, 1374 (1973); J. H. McGuire, At. Data and Nucl. Data Tables (to be published).
[10]D. H. Madison, A. B. Baskin, C. E. Busch, and S. M. Shafroth, Phys. Rev. A 9, 675 (1974).
[11]F. Abrath and T. Gray, Phys. Rev. A 9, 682 (1974).
[12]D. R. Bates and W. R. McDonough, J. Phys. B 5, L107 (1972); J. Phys. B 3, L83 (1970).
[13]J. M. Hansteen and O. P. Mosebekk, Z. Phys. 234, 281 (1970); J. Bang and J. M. Hansteen, K. Dan. Vidensk. Selsk. Mat-Fys. Medd. 31, No. 13 (1959).
[14]V. Fock, Z. Phys. 98, 145 (1935).